Proceedings of the IASTED International Conference
Control and Applications (CA 2011)
June 1 - 3, 2011 Vancouver, BC, Canada

DESIGN OF A NEW COMPOSITE OBSERVER FOR VEHICLE VELOCITY AND ATTITUDE ESTIMATION

Jiwon Oh, Seibum B. Choi
(Automotive Control Lab., Dept. of Mechanical Engineering)
Korea Advanced Institute of Science and Technology
373-1 Guseong-dong, Yuseong-gu, Republic of Korea
jwo@kaist.ac.kr

ABSTRACT
The main concern of this paper focuses on the accurate estimation of the vehicle states, including the longitudinal, lateral, and vertical velocities (hence, sideslip angle), as well as the roll and pitch angles. With the input data from the 6D IMU which measures both acceleration and angular velocities of the three axes, the novel merging schemes based on the internally defined concepts of transient state factor, reference selector, and selective integral, that combine the kinematic and model-based observer outputs guarantee robust performance in estimating the vehicle states. Stability of each component of the proposed observer is investigated, and confirmatory assessment of the entire system is arranged via simulation under various conditions, with the aid of Carsim and Matlab/Simulink.

KEY WORDS
Vehicle and transportation systems; identification and estimation; adaptation; stability; kinematics; linear bicycle model; side slip angle; vertical velocity; roll angle; pitch angle

1. Introduction

The worldwide proliferation of the automobile has brought efficiency and convenience at the cost of the unavoidable risk – car accidents of innumerable different types. This has encouraged the advancement of the electronic vehicle safety control technology, and the implementation of various computerized technologies has nowadays become vital. For example, the accurate knowledge of vehicle roll angle, side slip angle, and vertical velocity can significantly reduce the risk of rollover accidents through roll stability control (RSC), electronic stability program (ESP) and continuous damping control (CDC).

The main challenge in such implementation, however, lies in fact that the reliable sensors to accurately measure the necessary information about the vehicle states is not available at a cost affordable enough for production vehicles. While maintaining the cost of the utilized hardware affordable – implying that the uncertainty level of the sensor outputs may be higher than desired – the state estimation algorithm must ensure robust performance, even during the vehicle maneuvers which show highly nonlinear tire characteristic, and in the existence of road inclination or bank angle. Such requirements have served obstacles in the previous efforts to develop a wholly satisfactory vehicle state estimation algorithm [1][2][3][4][5][6][7][8][9][10].

This paper introduces an integrated vehicle state observer comprising a model-based observer that uses the linear bicycle model to estimate the lateral velocity, a kinematic velocity observer that uses the kinematics of motion to estimate the vehicle velocities of all three axes, an Euler angle observer that estimates the chassis pitch and roll, and merging schemes that effectively combine the outputs of the aforementioned subsystems. The choice to

Nomenclature

m : vehicle mass	δ_f : front tire steering angle	p : roll rate measured at C.G.
g : gravitational constant	β : side slip angle at C.G	q : pitch rate measured at C.G.
h : C.G. height	v_x : longitudinal velocity at C.G.	r : yaw rate measured at C.G.
l_f : distance between C.G. and front axle	v_y : lateral velocity at C.G.	F_{yf} : front axle lateral tire force
l_r : distance between C.G. and rear axle	v_z : vertical velocity at C.G.	F_{yr} : rear axle lateral tire force
L : distance between front and rear axle	a_x : longitudinal acceleration measured at C.G.	F_{zf} : front axle vertical tire force
I_y : moment of inertia about y-axis	a_y : lateral acceleration measured at C.G.	F_{zr} : rear axle vertical tire force
I_z : moment of inertia about z-axis	a_z : vertical acceleration measured at C.G	IC : integration cease cue
α_f : front tire slip angle	ϕ : roll angle	TF : transient state factor
α_r : rear tire slip angle	θ : pitch angle	SF : steady-state stability factor
C_f : front tire cornering stiffness	ψ : yaw angle	RS : reference selector
C_r : rear tire cornering stiffness		

DOI: 10.2316/P.2011.729-019

use a 6D IMU allows the estimation of the vertical velocity and vehicle pitch angle on top of the longitudinal and lateral velocity and roll angle. As a novel contribution of this paper, it must be also noted that the coexistence of the model-based and kinematic observer with the aid of cornering stiffness adaptation and an effectively designed merging scheme ensures robust estimation performance even during the vehicle maneuvers which show highly nonlinear tire characteristic. Such maneuvers include an oversteer motion or a J-turn with a complete spin out and a full wheel slip occurred from full braking unaided by ABS.

The basic organization of this paper is as follows. Section 2.1 contains information on the general layout of the observer with the data flow description. Section 2.2 denotes the principle behind the reference longitudinal velocity approximation. Section 2.3 describes the method of cornering stiffness adaptation based on the bicycle model. As section 2.4 focuses on the model-based velocity observer design, section 2.5 focuses on the alternative velocity observer based on the vehicle kinematics, and also on how the estimated results of the two observers are effectively affined. Section 2.6 describes the method to estimate the vehicle pitch and roll angles. To display the validity of the suggested observer, section 3 discusses the results of the simulation performed under various different scenarios.

2. Observer Design

2.1 General Observer Flow Chart

The general structure of the entire observer is as follows:

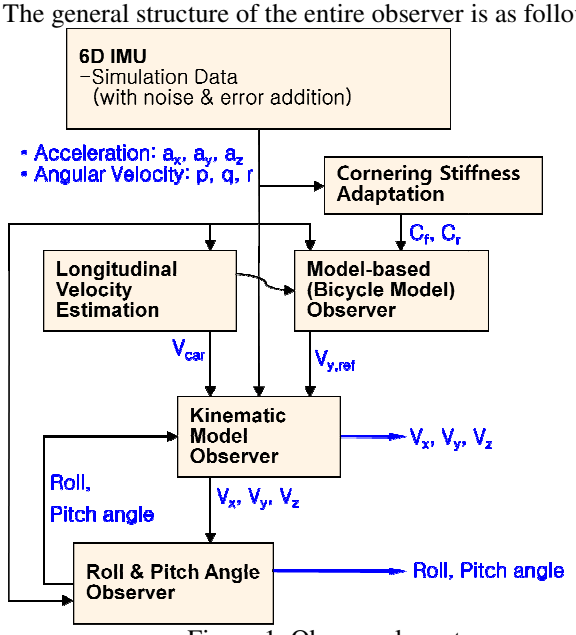

Figure 1. Observer layout

2.2 Longitudinal Velocity Estimation

Using the four wheel angular velocities available, a rough estimation of the longitudinal velocity is obtained. Using the undriven wheel speed during acceleration and the maximum wheel speed during deceleration, a low pass filter and a rate limiter are applied with taking the physical limitations of the vehicle into consideration. This estimation, v_{car}, is merely a reference value used in the other parts of the observer, and must be clarified that it is independent from the final output for the vehicle longitudinal velocity.

2.3 Cornering Stiffness Adaptation

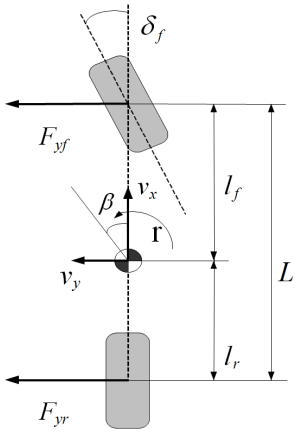

Figure 2. Bicycle model

Bicycle model represents the lateral dynamics of the vehicle, as shown in Figure 2. It is a simplified model of the full vehicle under an assumption that the longitudinal velocity of the vehicle is constant and that the tire cornering stiffness of the left and right side of the vehicle are equivalent. Although this model may be sensitive to the road surface condition change and discrepancies between the nominal and real vehicle parameters, it significantly reduces the amount of required calculation while maintaining fairly high accuracy. Moreover, being unconfined from having to directly use the lateral acceleration sensor provides robustness against sensor error.

Based on the bicycle model, it is possible to apply adaptive scheme for the front and rear tire cornering stiffness values [10]. From the moment balance equations, front and rear lateral tire forces can be defined as the following:

$$F_{yf} = \frac{ml_r a_y + I_z \dot{r}}{l_f + l_r}, F_{yr} = \frac{ml_f a_y - I_z \dot{r}}{l_f + l_r} \quad (1a)(1b)$$

Also, the front and rear tire slip angles can be derived as follows.

$$\alpha_f = \beta + \frac{l_f}{v_x} r - \delta_f, \alpha_r = \beta - \frac{l_r}{v_x} r \quad (2a)(2b)$$

The linear tire model is used to calculate the lateral forces related to the tire, and it exhibits the following relationship between the tire slip angle and lateral force.

$$F_{yf} = -C_f \alpha_f, F_{yr} = -C_r \alpha_r \quad (3a)(3b)$$

By substituting (2) into (3) and performing an algebraic manipulation, (4) is obtained.

$$\beta = -\frac{F_{yf}}{C_f} + \delta_f - \frac{l_f}{v_x} r, \beta = -\frac{F_{yr}}{C_r} + \frac{l_r}{v_x} r \quad (4a)(4b)$$

Since the side slip angle is an unknown variable, it is eliminated by equating (4a) and (4b), which gives

$$\frac{F_{yf}}{C_f}-\frac{F_{yr}}{C_r}=\delta_f-\frac{l_f+l_r}{v_x}r \tag{5}$$

Here, $\frac{1}{C_f}$ and $\frac{1}{C_r}$ are modelled as

$$\frac{1}{C_f}=\left(\frac{1}{C_f}\right)_n+z_f \text{ and } \frac{1}{C_r}=\left(\frac{1}{C_r}\right)_n+z_r \tag{6a)(6b}$$

where $\left(\frac{1}{C_f}\right)_n$ and $\left(\frac{1}{C_r}\right)_n$ are the nominal values,

and z_f and z_r are the unknown parts [10].

Substituting (6) into (5) leads to

$$F_{yf}\left(\left(\frac{1}{C_f}\right)_n+z_f\right)-F_{yr}\left(\left(\frac{1}{C_r}\right)_n+z_r\right)=\delta_f-\frac{l_f+l_r}{v_x}r \tag{7}$$

Now a variable z is defined as

$$\begin{aligned} z &\equiv \delta_f-\frac{l_f+l_r}{v_x}r-F_{yf}\left(\frac{1}{C_f}\right)_n+F_{yr}\left(\frac{1}{C_r}\right)_n \\ &= F_{yf}z_f-F_{yr}z_r \end{aligned} \tag{8}$$

and a low pass filter is applied to ensure that the system is causal.

$$\dot{z}=-\gamma z+F_{yf}z_f-F_{yr}z_r \tag{9}$$

Similarly, an estimated variable is defined as the following:

$$\dot{\hat{z}}=-\gamma\hat{z}+F_{yf}\hat{z}_f-F_{yr}\hat{z}_r \tag{10}$$

Using the following adaptation law for $\hat{z}_f$ and $\hat{z}_r$, the cornering stiffness can be estimated.

$$\dot{\hat{z}}_f=\gamma_f F_{yf}\varepsilon,\ \dot{\hat{z}}_r=-\gamma_r F_{yr}\varepsilon \tag{11a)(11b}$$

Stability of the system is easily proven. Define $\varepsilon=z-\hat{z}$, $\tilde{z}_f=z_f-\hat{z}_f$, and $\tilde{z}_r=z_r-\hat{z}_r$, with the radially unbounded, decrescent, and positive definite Lyapunov function as the following:

$$V=\frac{1}{2}\left(\varepsilon^2+\frac{\tilde{z}_f^{\,2}}{\gamma_f}+\frac{\tilde{z}_r^{\,2}}{\gamma_r}\right) \tag{12}$$

$$\begin{aligned} \frac{dV}{dt} &= \varepsilon\dot{\varepsilon}+\frac{\tilde{z}_f\dot{\tilde{z}}_f}{\gamma_f}+\frac{\tilde{z}_r\dot{\tilde{z}}_r}{\gamma_r}=\varepsilon\dot{\varepsilon}-\frac{\tilde{z}_f\dot{\hat{z}}_f}{\gamma_f}-\frac{\tilde{z}_r\dot{\hat{z}}_r}{\gamma_r} \\ &= \varepsilon\left(-\gamma\varepsilon+F_{yf}\tilde{z}_f-F_{yr}\tilde{z}_r\right)-F_{yf}\tilde{z}_f\varepsilon+F_{yr}\tilde{z}_r\varepsilon \\ &= -\gamma\varepsilon^2\le 0 \end{aligned} \tag{13}$$

Thus the system is asymptotically stable, given that F_{yf} and F_{yr} satisfy the PE condition [11].

2.4 Bicycle Model-Based Observer

The well-known equation for the bicycle model is given in the following.

$$\begin{aligned} \begin{bmatrix}\dot{\beta}\\ \dot{r}\end{bmatrix} &= \begin{bmatrix}a_{11} & a_{12}\\ a_{21} & a_{22}\end{bmatrix}\begin{bmatrix}\beta\\ r\end{bmatrix}+\begin{bmatrix}b_1\\ b_2\end{bmatrix}\delta_f \\ &= \begin{bmatrix}\frac{-2\left(C_f+C_r\right)}{mv_x} & \frac{-2\left(C_f l_f-C_r l_r\right)}{mv_x^{\,2}}-1\\ \frac{-2\left(C_f l_f-C_r l_r\right)}{I_z} & \frac{-2\left(C_f l_f^{\,2}+C_r l_r^{\,2}\right)}{I_z v_x}\end{bmatrix}\begin{bmatrix}\beta\\ r\end{bmatrix}+\begin{bmatrix}\frac{2C_f}{mv_x}\\ \frac{2C_f l_f}{I_z}\end{bmatrix}\delta_f \end{aligned} \tag{14}$$

Here, the cornering stiffness values obtained from the formerly shown adaptation scheme are fully utilized. Since the lateral acceleration can be expressed as

$$a_y=\dot{v}_y+rv_x, \tag{15}$$

algebraic manipulations lead to the (16) [8].

$$a_y=a_{11}v_x\beta+\left(a_{12}+1\right)v_x r+b_1 v_x\delta_f \tag{16}$$

For the sake of clarification, it must be noted that the a_y is the pure acceleration value, unaffected by the roll or pitch angle. In addition, the effect of the vertical motion is not considered, since its contribution is negligible. The following shows the output equation, which now incorporates the estimated values of the yaw rate and the lateral acceleration just mentioned.

$$\hat{y}=\begin{bmatrix}\hat{r}\\ \hat{a}_y\end{bmatrix}=\begin{bmatrix}0 & 1\\ a_{11}v_x & \left(a_{12}+1\right)v_x\end{bmatrix}\begin{bmatrix}\hat{\beta}\\ \hat{r}\end{bmatrix}+\begin{bmatrix}0\\ b_1 v_x\end{bmatrix}\delta_f \tag{17}$$

Using (17), the following observer design,

$$\dot{\hat{x}}=A\hat{x}+Bu+K\left(y-\hat{y}\right) \tag{18}$$

leads to the expanded expression,

$$\begin{aligned} \begin{bmatrix}\dot{\hat{\beta}}\\ \dot{\hat{r}}\end{bmatrix} &= \begin{bmatrix}a_{11}-K_2a_{11}v_x & a_{12}-K_1-K_2\left(a_{12}+1\right)v_x\\ a_{21}-K_4a_{11}v_x & a_{22}-K_3-K_4\left(a_{12}+1\right)v_x\end{bmatrix}\begin{bmatrix}\hat{\beta}\\ \hat{r}\end{bmatrix} \\ &+\begin{bmatrix}b_1-K_2b_1v_x\\ b_2-K_4b_1v_x\end{bmatrix}\delta_f+\begin{bmatrix}K_1 & K_2\\ K_3 & K_4\end{bmatrix}\begin{bmatrix}r\\ a_y\end{bmatrix} \end{aligned} \tag{19}$$

where $\hat{\beta}$ and $\hat{r}$ are the estimated side slip angle and yaw rate, respectively, whereas r and a_y are the measured yaw rate and the compensated lateral acceleration, respectively. The roll and pitch angle compensation of the lateral acceleration is dealt later in the paper.

The observer gain K is defined by the frozen-time pole-placement method in order to ensure system stability.

$$K=\begin{bmatrix}\frac{I_z\left(C_f l_f-C_r l_r\right)}{2C_f C_r\left(l_f+l_r\right)^2}p^2-1 & \frac{1}{v_x}\\ -2p & \frac{m\left(C_f l_f^{\,2}+C_r l_r^{\,2}\right)}{I_z\left(C_f l_f-C_r l_r\right)}\end{bmatrix}, \tag{20}$$

where p is a negative constant. It must be noted here, that for stability, K_2 and K_4 are made to zero when their denominators approach zero.

2.5 Kinematic Velocity Observer

The main concern of this paper focuses on the methodology to suitably make use of the kinematic observer along with the contribution of the model-based observer. Here, the kinematic observer involves the direct and full usage of the 6D IMU to obtain the vehicle velocities of three axes via integration. This may certainly involve issues of sensor error and drift due to integration. However, advantages regarding robust performance even with the vehicle parameter uncertainty and strongly nonlinear vehicle motion must be emphasized.

The kinematic equations of motion are expressed as the following,

$$\dot{v}_x = a_x + r \cdot v_y - q \cdot v_z + g \cdot \sin\theta \tag{21a}$$

$$\dot{v}_y = a_y - r \cdot v_x + p \cdot v_z - g \cdot \sin\phi \cdot \cos\theta \tag{21b}$$

$$\dot{v}_z = a_z + q \cdot v_x - p \cdot v_y - g \cdot \cos\phi \cdot \cos\theta \tag{21c}$$

and the proposed kinematic velocity observer is designed based on (21).

$$\begin{bmatrix} \dot{\hat{v}}_x \\ \dot{\hat{v}}_y \\ \dot{\hat{v}}_z \end{bmatrix} = TF\left\{ \begin{bmatrix} 0 & r & -q \\ -r & 0 & p \\ q & -p & 0 \end{bmatrix} \cdot \begin{bmatrix} \hat{v}_x \\ \hat{v}_y \\ \hat{v}_z \end{bmatrix} + \begin{bmatrix} a_x \\ a_y \\ a_z \end{bmatrix} \cdots \right.$$
$$\left. + g \begin{bmatrix} \sin\theta \\ -\sin\phi \cdot \cos\theta \\ -\cos\phi \cdot \cos\theta \end{bmatrix} + K_{ki} \cdot \begin{bmatrix} v_{car} - \hat{v}_x \\ v_{y,ref} - \hat{v}_y \\ 0 - \hat{v}_z \end{bmatrix} \right\} + SF \begin{bmatrix} \dot{v}_{car} \\ \dot{v}_{y,ref} \\ 0 \end{bmatrix} \tag{22}$$

$$\text{where } K_{ki} = \begin{bmatrix} k_1 & k_2 & k_3 \\ k_4 & k_5 & k_6 \\ k_7 & k_8 & k_9 \end{bmatrix} = \begin{bmatrix} \xi_x & r & -q \\ -r & \xi_y & p \\ q & -p & \xi_z \end{bmatrix}. \tag{23}$$

Here, ξ_x and ξ_z are positive constants,

and ξ_y is a time-varying pole for the estimation of $\hat{v}_y$.

$$\xi_y = c_y \cdot sat\left\{ \max\left(\frac{1}{2\varepsilon_t}\left(C_f - \Gamma_f F_{zf} + \varepsilon_t\right), \frac{1}{2\varepsilon_t}\left(C_r - \Gamma_r F_{zr} + \varepsilon_t\right) \right) \right\} + p_{\min} \tag{24}$$

Here, c_y and $p_{\min}$ are positive tuning parameters, and thus ξ_y satisfies the following.

$$p_{\min} \le \xi_y \le c_y + p_{\min} = p_{\max}. \tag{25}$$

Also, Γ_f, Γ_r, and ε_t are positive tuning parameters.

Here, neglecting the aerodynamic drag, the front and rear vertical tire forces can be readily calculated using the estimated vehicle states.

$$F_{zf} = \frac{mgl_r \cos\hat{\theta} - mgh\sin\hat{\theta} - mh\dot{\hat{v}}_x + ml_r\dot{\hat{v}}_z - I_y\dot{q}}{L}$$
$$F_{zr} = \frac{mgl_f \cos\hat{\theta} + mgh\sin\hat{\theta} + mh\dot{\hat{v}}_x + ml_f\dot{\hat{v}}_z + I_y\dot{q}}{L} \tag{26}$$

Through actively varying the pole, the observer can be induced to depend more heavily on the model-based estimation by increasing the pole, and also to depend more heavily on the kinematic estimation by doing the opposite.

The observer feedback term includes v_{car}, $v_{y,ref}$, and 0 as the reference velocities in x, y, and z directions, respectively. The formerly estimated longitudinal velocity v_{car} is used as the reference for x-axis kinematics. The reference vertical velocity is taken to be 0, since the mean vertical velocity over an extended period of time is equal to 0.

Now $v_{y,ref}$ is defined as the following:

$$v_{y,ref} = RS\left\{\hat{\beta}v_w\right\} + (1 - RS)\, v_{y,\text{int}} \tag{27}$$

The reference selector formulates $v_{y,ref}$ through merging the lateral velocity calculated using $\hat{\beta}$ obtained from the model-based observer, with $v_{y,\text{int}}$, another lateral velocity independently calculated by the selective integration of the lateral kinematics shown in (21b).

The reference selector is defined using the cornering stiffness adaptation formerly dealt.

$$RS = sat\left\{ \max\left(\frac{1}{2\varepsilon_t}\left(C_f - \Gamma_f F_{zf} + \varepsilon_t\right), \frac{1}{2\varepsilon_t}\left(C_r - \Gamma_r F_{zr} + \varepsilon_t\right) \right) \right\} \tag{28}$$

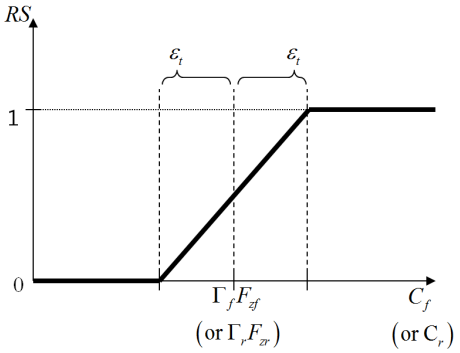

Figure 3. Reference selector acquisition

Figure 3. graphically represents how the reference selector is acquired. The threshold level is made to be a function of the vertical tire force, in order to compensate for the load transfer. The acquisition of ξ_y exhibits the similar principle as well. Since low cornering stiffness relative to the vertical forces indicates that the vehicle motion is more likely have nonlinear characteristics, the entire observer structure tends to rely more on the kinematics rather than the model parameters.

This explains the use of $v_{y,\text{int}}$ for the reference. However, integration using kinematics must be avoided as much as possible to prevent the estimation drift issue. Out of this dilemma has appeared the concept of selective integration. For the selective integration, the concept of the Boolean-type integration cease cue is introduced.

$$IC = \{RS > 0.5 \text{ OR } SF > 0.5\} \tag{29}$$

With $IC = 0$, the vehicle is likely to be going through a

motion which involves a highly nonlinear tire characteristic. Only when this is the case, (21b) is integrated to give $v_{y,\text{int}}$. Otherwise, integration stops and the lingering value of $v_{y,\text{int}}$ quickly returns back to the current $\hat{\beta}v_w$. A forgetting factor is additionally applied to prevent potential drift issue in case the vehicle tire exhibits nonlinear characteristic for an extended period of time, such as constant under/oversteering or spin out.

Apart from the reference selector, the transient state factor / steady state stability factor must be defined to discriminate the case in which the vehicle motion goes through the transient state but still majorly involves the linear tire characteristic. In this case, both the model-based and kinematic estimations are important for the sake of estimation accuracy. Also, these factors are required to swiftly correct the estimated observer outputs without going through integration, so that the issue concerning the sensor error is resolved. A high transient state factor continues the operation of the entire kinematic observer shown in (22), whereas a high steady state stability factor stops it.

$$TF = \begin{cases} sat\left(\dfrac{b_8\int_t^{t+\Delta t_8} x_7\ d\tau}{\Delta t} - \sigma_{v_x}\right) & \text{, nonlinear condition} \\ sat\left\{sat\left(\dfrac{b_8\int_t^{t+\Delta t_8} x_7\ d\tau}{\Delta t} - \sigma_{v_x}\right)\right\}\times\cdots & \\ \sum_{i=1}^{7}\left\{\dfrac{b_i\int_t^{t+\Delta t_i}\left(x_i - \dfrac{\int_t^{t+\Delta t_i} x_i\ d\tau}{\Delta t}\right)^2 d\tau}{\Delta t}\right\} & \text{, otherwise} \end{cases} \tag{30a}$$

$$SF = 1 - TF \tag{30b}$$

where $x_1 = a_x$, $x_2 = a_y$, $x_3 = a_z$, $x_4 = p$, $x_5 = q$, and $x_6 = r$, all measured by the sensor, $x_7 = v_{car}$, obtained from the v_{car} estimation, and b_i are positive tuning coefficients for each corresponding weight factor. b_8 and σ_{v_x} are also positive tuning coefficients to ensure that $TF = 0$ when $v_{car} = 0$ for a time period Δt_8, since there is a rare chance to require vehicle states estimation when the vehicle definitely has no longitudinal motion.

Nonlinear condition mentioned in (30) is defined as the state when either one of the following applies:

$$\text{(a)}\ \frac{\int_t^{t+\Delta t_9}\left(C_f - \dfrac{\int_t^{t+\Delta t_9} C_f\ d\tau}{\Delta t}\right)^2 d\tau}{\Delta t} > \sigma_{C_f} \tag{31}$$

$$\text{(b)}\ \frac{\int_t^{t+\Delta t_{10}}\left(C_r - \dfrac{\int_t^{t+\Delta t_{10}} C_r\ d\tau}{\Delta t}\right)^2 d\tau}{\Delta t} > \sigma_{C_r} \tag{32}$$

$$C_f < \eta_f\left(\left(\frac{1}{C_f}\right)_n\right)^{-1} \text{ or } C_r < \eta_r\left(\left(\frac{1}{C_r}\right)_n\right)^{-1}$$

$$\text{(c)}\ \text{when}\ \frac{\int_t^{t+\Delta t_{11}}\left(\delta_f - \dfrac{\int_t^{t+\Delta t_{11}} \delta_f\ d\tau}{\Delta t}\right)^2 d\tau}{\Delta t} > \sigma_{\delta_f} \tag{33}$$

where σ_{C_f}, σ_{C_r}, and σ_{δ_f} are positive tuning parameters, and η_f, η_r are the constants satisfying $0<\eta_f<1$ and $0<\eta_r<1$. In physical sense, (31) and (32) each corresponds to the case when the cornering stiffness values are significantly varying, and (33) corresponds to the case when the cornering stiffness values are lower than the threshold indicated. The term in (33) that includes δ_f is attached to ensure the PE condition for the sake of C_f and C_r adaptation validity. Even intuitively it is for certain that the tire is going through a nonlinear motion when the variance of the cornering stiffness values are high, or when they are low with high steering angle variance.

Stability of the kinematic vehicle observer can be easily verified, with the provision of the stability of the model-based observer. Knowing that v_{car}, the longitudinal velocity calculated based on the wheel angular velocities cannot drift off, and that $v_{y,ref}$ converges to the true lateral velocity when $RS > 0.5$ or $SF > 0.5$, the error dynamics is asymptotically stable, as long as

$$\begin{bmatrix} 0 & r & -q \\ -r & 0 & p \\ q & -p & 0 \end{bmatrix} - K_{ki}I \tag{34}$$

is Hurwitz. This claim is true, since

$$\begin{bmatrix} 0 & r & -q \\ -r & 0 & p \\ q & -p & 0 \end{bmatrix} - \begin{bmatrix} \xi_x & r & -q \\ -r & \xi_y & p \\ q & -p & \xi_z \end{bmatrix} = \begin{bmatrix} -\xi_x & 0 & 0 \\ 0 & -\xi_y & 0 \\ 0 & 0 & -\xi_z \end{bmatrix} \tag{35}$$

is Hurwitz for (23) and (25).

2.6 Euler Angle Observer

The Euler angle observer estimates the roll and pitch angles of the vehicle, based on the kinematics law for the Euler angle derivatives.

$$\dot{\phi} = p + \left(q\cdot\sin\phi + r\cdot\cos\phi\right)\cdot\tan\theta \tag{36a}$$

$$\dot{\theta} = q\cdot\cos\phi - r\cdot\sin\phi \tag{36b}$$

With the addition of the observer feedback and the reference term for the steady state, a new observer is designed, motivated by [12].

$$\dot{\hat{\phi}} = TF\begin{Bmatrix} p+(q\cdot\sin\phi + r\cdot\cos\phi)\cdot\tan\theta \\ +2\alpha|r|\left(\phi_{ref}-\hat{\phi}\right)\end{Bmatrix} + SF\cdot\dot{\phi}_{ref} \quad (37a)$$

$$\dot{\hat{\theta}} = TF\begin{Bmatrix} q\cdot\cos\phi - r\cdot\sin\phi \\ +\left(\alpha^2-1\right)r\left(\theta_{ref}-\hat{\theta}\right)\end{Bmatrix} + SF\cdot\dot{\theta}_{ref} \quad (37b)$$

Here,

$$\phi_{ref} = RS\left\{\sin^{-1}\left(\frac{-\dot{\hat{v}}_y + a_y - r\cdot\hat{v}_x + p\cdot\hat{v}_z}{g\cdot\cos\theta}\right)\right\} + (1-RS)\phi_{\text{int}} \quad (38a)$$

$$\theta_{ref} = RS\left\{\sin^{-1}\left(\frac{\dot{\hat{v}}_x - a_x - r\cdot\hat{v}_y + q\cdot\hat{v}_z}{g}\right)\right\} + (1-RS)\theta_{\text{int}} \quad (38b)$$

and θ_{int} , ϕ_{int} are the selective integral of the angle kinematics shown in (36), employing the same integration cease cue dealt in (29). The reference selector combines the reference angle primarily obtained from the algebraic manipulation of the kinematic laws shown in (21a) and (21b), with θ_{int} and ϕ_{int} . Because the error can be amplified, especially through taking the derivative, the reference selector rather lets the selectively integrated angles to be used as the reference for the angle observer, in case of the high kinematic observer dependency. Additionally, to prevent spoilage of the estimated angles due to a fast change in TF , a rate limiter that utilizes the measured roll rate (or pitch rate) value with tolerance as the reference is applied to $\hat{\phi}$ (or $\hat{\theta}$).

The estimated roll and pitch angles are used in the model-based observer for the compensation of the lateral acceleration shown in (17), and in the kinematic velocity observer for the elimination of the effect of gravity shown in (22).

As far as the stability is concerned, given that ϕ_{ref} and θ_{ref} are stable, the error dynamics of the observer is asymptotically stable as long as the error dynamics of the system

$$\dot{\hat{\phi}} = p + (q\cdot\sin\phi + r\cdot\cos\phi)\cdot\tan\theta + 2\alpha|r|\left(\phi_{ref}-\hat{\phi}\right) \quad (39a)$$

$$\dot{\hat{\theta}} = q\cdot\cos\phi - r\cdot\sin\phi + \left(\alpha^2-1\right)r\left(\theta_{ref}-\hat{\theta}\right) \quad (39b)$$

is stable, which is dealt in [12] assuming that the actual roll and pitch angles are small.

3. Simulation Results

Using CarSim, which is a well-known vehicle simulation tool, different scenarios involving diverse vehicle maneuvers and road characteristics are arranged as shown in Table 1. A mid-size front wheel drive passenger car is used for simulation, and the vehicle parameters are as follows:

$m = 1370\ kg,\ h = 0.536\ m,\ l_f = 1.110\ m,\ l_r = 1.66622\ m,$

$I_y = 2851\ kg\cdot m^2,\ I_z = 4192\ kg\cdot m^2,$

$\left(\frac{1}{C_f}\right)_n = \frac{\pi}{2000\cdot 180}\ rad\cdot N^{-1},\ \left(\frac{1}{C_r}\right)_n = \frac{\pi}{1600\cdot 180}\ rad\cdot N^{-1}$

In each of the cases, the suggested algorithm is applied to estimate the vehicle states, and each estimated states are compared to the true value provided by CarSim. It must be noted that, instead of simply using the ideal 6D IMU sensor signals provided by CarSim, the sensor bias errors and noises of 3 deg/s and 0.2 deg/s (RMS based) for gyroscopes and 0.25m/s^2 and 0.02 m/s^2 (RMS based) for accelerometers are deliberately added to verify the estimation performance under the influence of sensor inaccuracy.

Case	Driver Control	Bank [%]	Incline [%]	v_x [kph]	Road friction
Case I	Double lane change	none	none	40	0.25
Case II	Double lane change	none	0→3→ -3→0	80	0.85
Case III	Double lane change	0→15→0	irregular (bumpy)	80	0.85
Case IV	Sine steer	0→15→0	none	80	0.85
Case V	J-turn	0→15→0	none	80	0.25

Table 1

Case I.

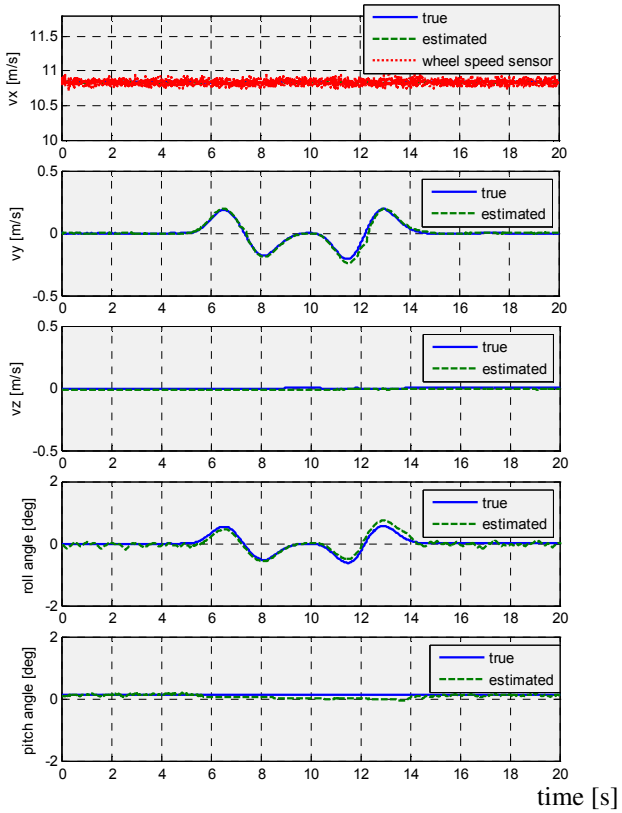

Figure 4

Case II

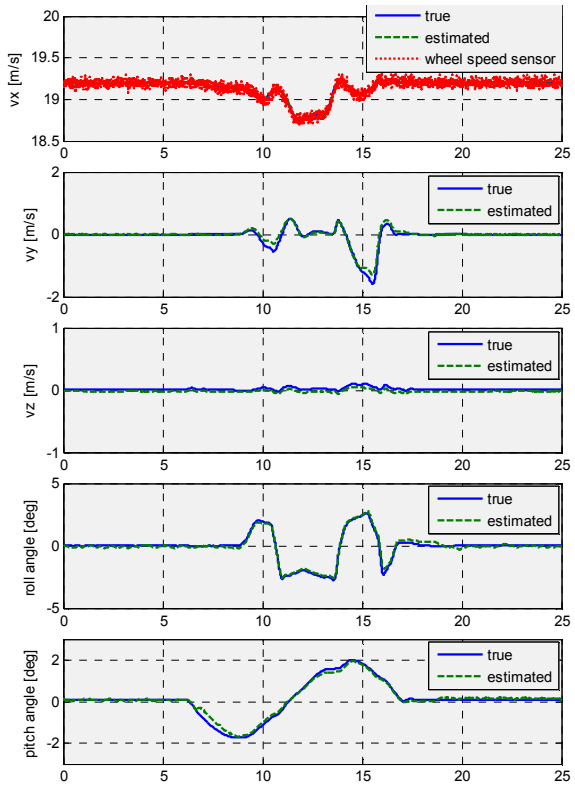

Figure 5

Case III

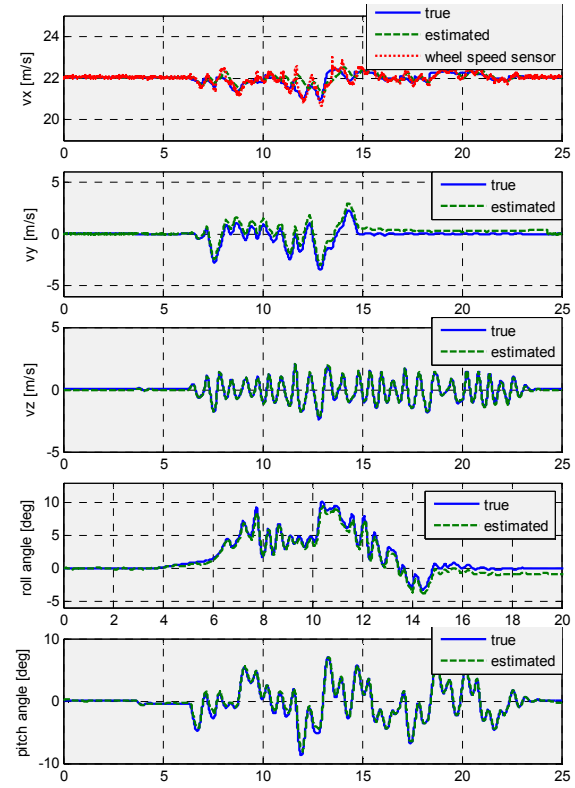

Figure 6

Case IV

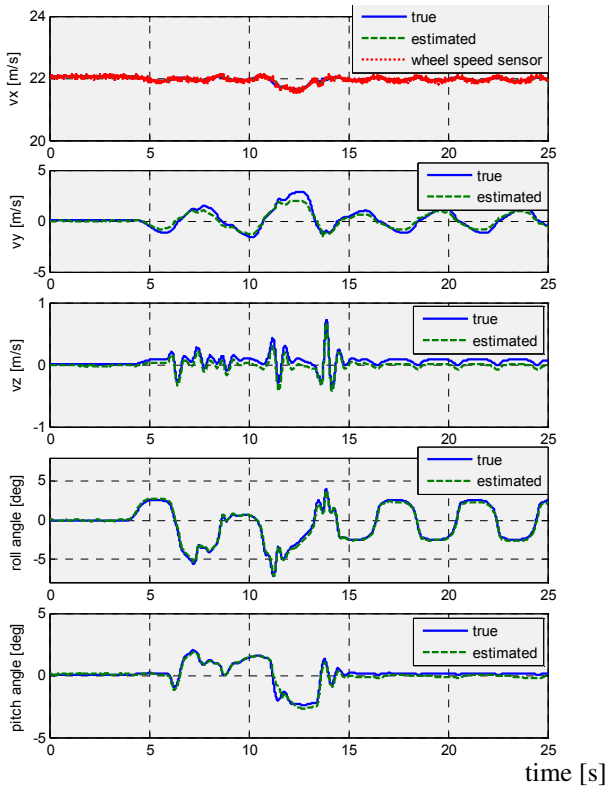

Figure 7

Case V

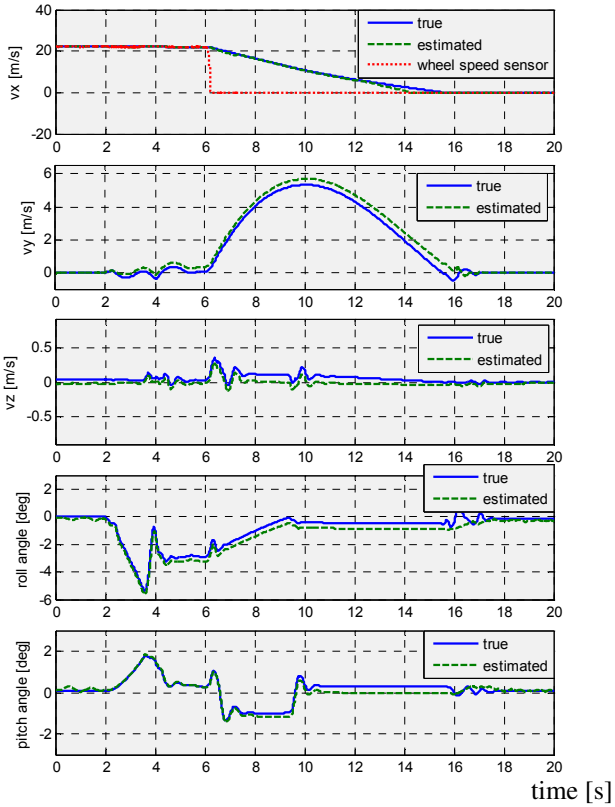

Figure 8

Generally, from Case I to Case V, the vehicle motion involves increasing tire nonlinearity with greater lateral velocity. Even when the vehicle is completely sliding sideway in Case V, it is observed that the estimation algorithm effectively tracks the lateral motion. Also, the suggested observer estimates the vehicle states even during the transient state with varying pitch and roll angles fairly accurately, when there is bank or inclination angle of the road.

It can be seen in Figure 5 that a significantly high amount of roll angle is observed, and it is indeed justified since lateral maneuvers on the inclined road should create bank angle from the vehicle frame of reference. As shown in Figure 6 to 8, the same applies to Case III to V where the vehicle orientation on the bank angle influences the pitch.

Although the estimation result for the lateral velocity may not cleanly track the true value in case frequent switching between the model-based and kinematic observer dependency occurs as shown in Figure 7, the result generally shows a tendency to follow the desired value with reasonable accuracy. Also, studying the plot for the longitudinal velocity in Figure 8 reveals the advantage of estimating the longitudinal velocity with the aid of the kinematic observer, since the estimated longitudinal velocity accurately follows the true one despite the full braking that already had caused the wheels to lock completely.

4. Conclusion

An original method to combine the use of the model-based observer and kinematic observer is proposed. Making use of the inexpensive 6D IMU, the proposed observer shows a robust estimation performance, even under the influence of sensor error and nonlinear tire characteristic. Summarizing the paper, the original contributions distinguished from the previously reported papers are the following: the ability to estimate the vehicle velocities of all three axes both in transient and steady states, through the design of internal parameters for observer merging, the robust estimation performance in both linear and highly nonlinear region for tire characteristic, and the ability to estimate the vehicle pitch and roll angles both in transient and steady states.

References

[1] J. Farrelly, P. Wellstead, Estimation of Vehicle Lateral Velocity, *Proceedings of the 1996 IEEE International Conference on Control Applications*, Dearborn, MI, 1996, 552~557.

[2] Y. Fukada, Slip-angle Estimation for Vehicle Stability Control, *Vehicle System Dynamics*, 1999, Vol. 32, 375~388.

[3] J. Hahn, R. Rajamani, S. You, K. Lee, Road bank angle estimation using disturbance observer, *Proceedings of the 6th international Symposium on AVEC*, 2002, 381~386.

[4] M. Kaminaga, G. Naito, Vehicle Body Slip Angle Estimation using an Adaptive Observer, *Proceeding of the Int. Symposium on Advanced Vehicle Control*, 1998, 207~212.

[5] C.S. Liu & H. Peng, A state and parameter identification scheme for linearly parameterized systems, *ASME Journal of Dynamic Systems, Measurement and Control*, 1998, 120, 524–528.

[6] H.E. Tseng, Dynamic Estimation of Road Bank angle, *Vehicle System Dynamics,* 2001, Vol. 36, No. 4~5, 307~328.

[7] H.E. Tseng, A sliding model lateral velocity observer, In Proceedings of the international symposium on advanced vehicle control, 2002, 387–392.

[8] H.W. Son, A Study on Design of a Robust Vehicle Side-Slip Angle Observer using an Integration of Kinematic and Bicycle Model, *KSAE 2008 Annual Conference*, Daejeon, Korea, 2008.

[9] A.Y. Ungoren, H. Peng, H.E. Tseng, A study on lateral speed estimation methods, *Int. J. Vehicle Autonomous Systems*, Vol. 2, 2004, 126~144.

[10] S.H. You, J.O. Hahn, H.C. Lee, New Adaptive Approaches to Real-time Estimation of Vehicle Sideslip Angle, *Control Engineering Practice*, 17 (12), 2009, 1367–1379.

[11] P.A. Ioannou, J. Sun, *Robust adaptive control* (Englewood Cliffs, NJ: Prentice-Hall, 1996).

[12] H.E. Tseng, L. Xu, D. Hrovat, Estimation of Land Vehicle Roll and Pitch Angles, *Proceeding of the 8th Int. Symposium on Advanced Vehicle Control*, Taipei, Taiwan, 2006, 445–450.